

Sustainable exploitation of residual *Cynara cardunculus* L. to levulinic acid and *n*-butyl levulinate

Anna Maria Raspolli Galletti ^{1,*}, Domenico Licursi ¹, Serena Ciorba ¹, Nicola Di Fidio¹, Valentina Coccia ², Franco Cotana ² and Claudia Antonetti ¹

¹ Department of Chemistry and Industrial Chemistry University of Pisa, Via Giuseppe Moruzzi 13, 56124 Pisa, Italy;

² CIRIAF, CRB Section (Biomass Research Center), Department of Engineering, University of Perugia, Via G. Duranti 67, 06125 Perugia, Italy;

* Correspondence: anna.maria.raspolli.galletti@unipi.it; Tel.: +39- 50- 2219290 (A.M.R.G.)

Abstract: Hydrolysis and butanolysis of lignocellulosic biomass are efficient routes to produce two valuable bio-based platform chemicals, such as levulinic acid and *n*-butyl levulinate, which find increasing applications in the field of bio-fuels, for the synthesis of intermediates for chemical and pharmaceutical industries, food additives, surfactants, solvents and polymers. In this research, the acid-catalyzed hydrolysis of the waste residue of *Cynara cardunculus* L. (cardo), remaining after seeds removal for oil exploitation, was investigated. The cardoon residue was employed as-received and after a steam-explosion treatment which causes an enrichment in cellulose. The effect of the main reaction parameters, such as catalyst type and loading, reaction time, temperature and heating methodology, on the hydrolysis process was assessed. Levulinic acid molar yields up to about 50 mol% with levulinic acid concentrations of 62.1 g/L were reached. Moreover, the one-pot butanolysis of the steam-exploded cardoon with the bio-alcohol *n*-butanol was investigated, demonstrating the direct production of *n*-butyl levulinate with good yield, up to 42.5 mol%. These results demonstrate that such residual biomass represents a promising feedstock for the sustainable production of levulinic acid and *n*-butyl levulinate, opening the way to the complete exploitation of this crop.

Keywords: cardoon; waste biomass; hydrolysis; levulinic acid; alcoholysis; *n*-butyl levulinate; bio-fuels; microwaves.

Citation: Lastname, F.; Lastname, F.; Lastname, F. Title. *Catalysts* **2021**, *11*, x. <https://doi.org/10.3390/xxxxx>

Academic Editor: Firstname Lastname

Received: date

Accepted: date

Published: date

Publisher's Note: MDPI stays neutral with regard to jurisdictional claims in published maps and institutional affiliations.



Copyright: © 2021 by the authors. Submitted for possible open access publication under the terms and conditions of the Creative Commons Attribution (CC BY) license (<http://creativecommons.org/licenses/by/4.0/>).

1. Introduction

Renewable resources have garnered increasing interest due to the shortage of petroleum, recurring rise in its price and environmental deterioration associated with its consumption, including pollutant by-products and greenhouse gases emission. The serious need to explore alternative resources respect to traditional ones for the production of chemicals and fuels has encouraged a new, more aware international policy of energy and economy. The European Union has recently incremented the amount of the renewable component of fuels and also the Italian legislation requires that 10% of fuels on sale in Italy to be made of bio-fuel by 2020 [1,2]. The use of the waste biomass for energy purposes, instead of fossil fuels, should reduce the greenhouse effect, since biomass releases the same amount of carbon dioxide which has been previously trapped from atmosphere during photosynthesis. Additionally, it is worthy of notice that methane, a 25 times more powerful greenhouse gas than carbon dioxide, is emitted during the decomposition of organic material in landfills [3,4]. In this scenario, not only the simple thermal-valorization but also the chemical conversion of non-edible biomass to exploitable bio-molecules should be developed and implemented, possibly avoiding any conflict with the food chain. In this regard, the ability to employ residual or waste biomasses as starting materials using water or a bio-alcohol as reactants/reaction media represents an added value that fits well with the concept of green chemistry. In this context a growing interest is recently dedicated to third-generation infesting plant species, such as the *Cynara cardunculus* (cardoon). It represents a promising resource to produce bio-materials and bio-chemicals and is a very common variety in the Center of Italy and in the Mediterranean Region [5]. *Cynara cardunculus* L. offers a wide spectrum of potential applications, being a rich source of fibers, oils and bioactive compounds [6,7]. Interestingly, the cultivation of such perennial herbaceous biomass shows significant advantages, such as good adaptability to climate change and growth on marginal or uncultivated lands with modest inputs, including little irrigation, care and minimal need of nutrients [8]. The seeds of the flower are exploited for oil production in food and bio-diesel supply chains. On the other hand, the non-edible lignocellulosic residues of this crop are reduced to a size of 20-40 mm by chipping and/or can undergo pre-treatments that favor further exploitation of this biomass [9,10]. Steam-explosion is the most common and cost-effective method for pre-treatment of lignocellulosic materials [11,12]. According to this process, chipped biomass is treated with high-pressure saturated steam for a few minutes at initial temperatures of 160-260°C, corresponding to a pressure of 0.69–4.83 MPa, then the pressure is rapidly reduced, thus leading to explosive decompression of the biomass and fibers damage. The process causes hemicellulose degradation and lignin transformation, due to high employed temperatures, and, in addition, it reduces the cellulose crystallinity, thus increasing the effectiveness of an eventual subsequent cellulose valorization.

In the present research, two types of cardoon waste residues, remaining after seeds removal, were studied: the first one is the un-treated defatted biomass, whereas the second one is the waste residue recovered after a steam-explosion pre-treatment.

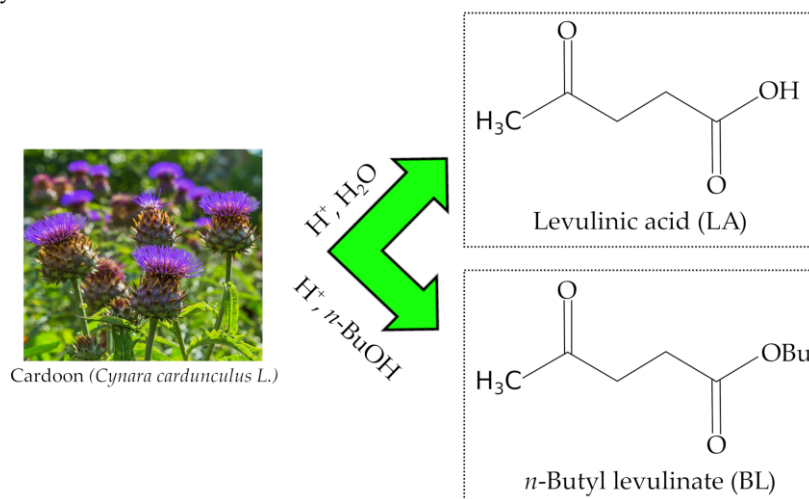
The hydrolysis of the cellulosic fraction of lignocellulosic biomass represents an efficient way to produce valuable platform chemicals, such as levulinic acid (LA) [13]. This last has been highlighted by the United States Department of Energy in 2010 as one of the 10 most promising building blocks in chemistry [14]. Due to its carboxyl and carbonyl functionalities, LA can be converted into various products for large-volume chemical markets, as bio-fuels, intermediates for chemical and pharmaceutical industries, food additives, surfactants, solvents and polymers [15]. In particular, the most promising LA derivatives for bio-fuels production are its alkyl esters, i.e. alkyl levulinates, γ -valerolactone, 2-methyltetrahydrofuran [16-19]. The LA yield is strongly affected by the cellulose content of the adopted feedstock [6,13] which can be changed by applying pre-treatments [20]. Taking into consideration that LA is produced via hydrolysis of hexose sugars (glucose, fructose, mannose and galactose), cellulose-rich biomass results the most suitable feedstock for its production [21].

30
31
32
33
34
35
36
37
38
39
40
41
42
43
44
45
46
47
48
49
50
51
52
53
54
55
56
57
58
59
60
61
62
63
64
65
66
67
68
69
70
71
72
73
74
75
76
77
78
79
80
81
82
83

The acid-catalyzed hydrolysis, assisted by microwave (MW) irradiation, was successfully performed for the two different samples of residual *Cynara cardunculus* L. and the effect of the main reaction parameters was investigated. Taking into account the high reached LA concentration, the hydrolysis of steam-exploded cardoon was also performed in a batch autoclave, in the perspective of a larger scaling-up.

In addition, the direct production of *n*-butyl levulinate (BL) by alcoholysis with *n*-butanol of the cellulose-rich steam-exploded biomass was also studied and discussed, being this strategy more promising than the generally adopted procedure of esterification of neat levulinic acid [22]. Indeed, the one-pot synthesis does not require intermediate operations concerning LA concentration and purification and reduces also the waste water treatment [23-25]. BL finds interesting applications not only as solvent and intermediate, but also as valuable bio-blendstock for diesel fuel, being able to reduce the emissions of particulate without increasing NO_x emissions or worsening engine performances respect to the neat conventional diesel fuel [25].

In Scheme 1 the two described approaches of valorization of cardoon by hydrolysis and alcoholysis are shown.



Scheme 1: Different hydrolysis and alcoholysis approaches of valorization of defatted *Cynara cardunculus* L. employed in the present research.

In the perspective of complete exploitation of the starting biomass, the solid residues recovered at the end of the hydrolysis and alcoholysis reactions were characterized by FT-IR spectroscopy, thermogravimetric and elemental analysis.

The obtained results of both hydrolysis and butanolysis runs highlight cardoon as a promising feedstock for multi-products biorefineries. A notable example of third-generation biorefinery fed by cardoon is represented by the industrial site in Porto Torres (Italy). Novamont S.p.A. and ENI Versalis S.p.A. converted a petrochemical refinery into an integrated green chemicals plant, which involves local agriculture, including cultivation of cardoon and, currently, the production site is dedicated to bio-plasticizers and bio-lubricants [26]. However, a new challenge for this innovative biorefinery is to integrate the manufacturing processes also with the synthesis of LA and ALs from the residual defatted biomasses, due to the excellent applicative perspectives of these bioproducts.

2. Results and Discussion

2.1 Compositional analysis of crude cardoon samples

The chemical compositions of the two investigated biomasses, the un-treated defatted cardoon residue (C) and the same biomass recovered after a steam-explosion pre-treatment (E), are reported in Figure 1.

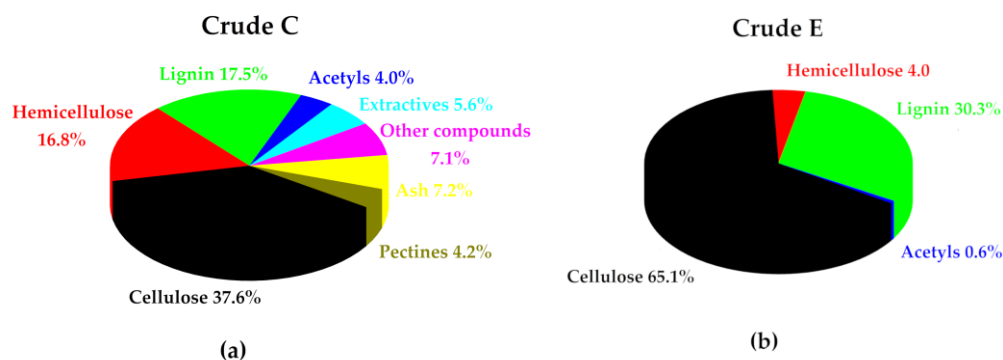


Figure 1. Chemical compositions of un-treated cardoon residue (C) and the same biomass recovered after a steam-explosion pre-treatment (E), reported as wt%, on dry basis.

The steam-explosion pretreatment is a high pressure and temperature physical process that has been largely experienced for biomasses in the last decades [27] since it allows increased availability of cellulose of the raw lignocellulosic matrix for further processing. The possible use of steam-exploded pretreated biomass is on one hand the production of bioethanol or more in general energy carriers [28] and on the other hand the possibility to obtain high value biochemical, such as the nanocrystalline cellulose [5] and other products useful for several chemical or pharmaceutical applications. The input matrices to the steam-explosion pretreatment section can be lignocellulosic softwoods, hardwoods and spruces but also residues obtained from agro-industrial activities, such as tomatoes, vineyard pruning or residues of infesting species, such as the *Cynara cardunculus* that can be considered third-generation biomass of growing interest for the production of sustainable biomaterials [29]. The process “intensity” is generally described by the severity factor (R₀) that considers the process parameters, such as the temperature and the pressure. In the case of lignocellulosic materials, the process yields can be significantly increased using a double-step process of both solid and liquid fraction after the pretreatment [28]. The steam-explosion facility used for this research is available at the University of Perugia (CRB/CIRIAF) and it is composed of: (i) vapor generator; (ii) charging section for raw biomass; (iii) expansion valves; (iv) high-pressure reactor; (v) post-explosion tank and (vi) exploded liquid recovery section [28].

Both C and E samples show very different content of cellulose, about 38 and 65 wt%, respectively. In fact, after the steam-explosion pre-treatment, the hemicellulose amount decreased from about 17 to 4 wt%, whereas extractives and ash were removed, as expected. On the other hand, lignin increased from about 17 up to 30 wt%, due to the reduction of the content of other components. The above-reported composition was determined on the dry biomasses; the available defatted raw sample C has a humidity amount of 5.9 wt %, while, as expected, the steam-exploded sample E has a humidity level of 73.6 %. Both wet as-received samples and dried ones were tested in the catalytic runs.

2.2 MW-assisted hydrolysis of C and E cardoon samples

A preliminary study on the effect of the catalyst types, their amount and humidity on LA formation was performed. The hydrolysis of dry cardoon, both C and E samples,

was carried out using two acid catalysts, HCl and H₂SO₄. The amount of these mineral acids was calculated to have the same concentration of hydronium ions in the starting mixtures. Table 1 reports the results for the experiments performed employing a biomass loading of 10 wt% (on dry basis), working at 190°C for 20 minutes in the MW reactor.

Table 1. Hydrolysis experiments of C and E cardoon samples with different type and amount of catalysts and humidity grade. Experimental conditions: 190°C, 20 min, biomass loading = 10 wt% (on dry basis), MW heating.

Run	Catalyst (wt%)	sub/cat (mol/mol) ^a	Products (g/L) ^b				LA ponderal yield (wt%)	LA molar yield (mol%)
			Glu	AA	FA	LA		
C1 (dry) ^c	HCl (1.6 wt%)	0.9	0.2	5.6	8.2	15.5	13.3	49.3
C2 (dry) ^c	H ₂ SO ₄ (2.1 wt%)	1.8	0.1	6.0	7.1	13.0	11.2	41.5
E1 (dry) ^c	HCl (1.6 wt%)	0.9	0.1	-	7.9	26.9	23.0	48.4
E2 (dry) ^c	H ₂ SO ₄ (2.1 wt%)	1.8	0.5	-	7.1	22.5	19.3	40.7
C3 (wet) ^d	HCl (1.6 wt%)	0.9	0.2	5.6	8.5	15.9	13.6	50.7
E3 (wet) ^d	HCl (1.6 wt%)	0.9	0.1	-	9.4	25.5	23.6	49.7

^a substrate to catalyst molar ratio: mol of anhydrous glucose unit in the starting biomass/mol of catalyst; ^b Glu = glucose; AA = acetic acid; FA = formic acid; ^c the sample was used after drying step; ^d the sample was employed as received.

In the presence of HCl, both dry samples (runs C1 and E1, Table 1) achieve comparable LA yields, 49.3 and 48.4 mol% respectively. Adopting the same dry samples, when H₂SO₄ was used (runs C2 and E2), lower LA molar yields were obtained, 41.5 and 40.7 mol% for C and E cardoon samples, respectively. As reported in previous studies, HCl enhances LA hydrolysis via a one-pot mechanism, since Cl⁻ ions catalyze the intermediate 5-hydroxymethyl-2-furaldehyde (HMF) re-hydration reaction, while SO₄²⁻ ions are responsible for an inhibitor effect [30]. In all these runs, low amounts of unconverted glucose were detected, while no intermediates, such as furfural and HMF, were observed. On the other hand, appreciable amounts of formic acid (FA), which is another commodity chemical [8], were co-formed by the hydrolysis of both C and E cardoon samples. Indeed, FA is co-produced during biomass hydrolysis [31] and its use in several fields has further encouraged the interest in LA synthesis. In our experiments, FA formation seems to be slightly facilitated when HCl is employed (compare runs C1 with C2 and runs E1 with E2) and for this reason, only HCl was selected for the subsequent investigation regarding the humidity grade. To investigate this parameter, both the cardoon samples C and E were adopted as-received with the humidity grade of 5.9 and 73.6 wt% respectively (runs C3 and E3), using the same experimental conditions of runs C1 and E1. As expected, dry and wet cardoon samples show similar LA molar yields, which are 49.3 and 50.7 mol% for dry and wet C (runs C1 and C3), respectively, and 48.4 and 49.7 mol% for dry and wet E (runs E1 and E3), respectively. Based on these results, since wet biomass can be directly used, only as-received wet cardoon samples were employed for a more detailed investigation. In the perspective of industrial application, the adoption of a high biomass loading is to be preferred, thus applying the *High Gravity* approach to achieve the highest products concentration. Such a method presents several advantages for an industrial perspective: it increases the concentration of crude products, reduces the costs

for their purification and waste-water treatment. On the other hand, in an over-loaded reactor, a more difficult physical agitation of the reaction slurry could lead to a significant decrease in the reaction rate. Table 2 reports the results of hydrolysis experiments carried out by increasing the biomass loading from 10 up to 20 wt% on dry basis, keeping constant the other reaction parameters (190°C, 20 minutes, HCl as catalyst). In the same Table 2, the effect of the substrate to catalyst ratio was investigated at 20 wt% of biomass loading, for both wet C and E cardoon samples.

Table 2. Hydrolysis experiments on wet C and E cardoon samples with different biomass loadings and substrate/catalyst molar ratios. Experimental conditions: 190°C, 20 min, HCl as catalyst, MW heating.

Run	Biomass loading (wt%) ^a	sub/cat (mol/mol) ^b (HCl wt%)	Products (g/L) ^c				LA ponderal yield (wt%)	LA molar yield (mol%)
			Glu	AA	FA	LA		
C3	10	0.9 (1.6 wt%)	0.2	5.6	8.5	15.9	13.6	50.7
C4	15	0.9 (2.4 wt%)	0.5	8.6	12.7	23.9	13.0	48.1
C5	20	0.9 (3.2 wt%)	-	9.3	12.7	34.6	13.0	48.5
C6	20	1.5 (1.9 wt%)	-	9.7	13.4	27.8	10.7	39.8
C7	20	2.0 (1.4 wt%)	-	7.5	12.7	34.3	13.3	49.6
E3	10	0.9 (1.6 wt%)	0.1	-	9.4	25.5	23.6	49.7
E4	15	0.9 (2.4 wt%)	-	-	11.7	47.0	24.6	51.8
E5	20	0.9 (3.2 wt%)	-	-	12.5	58.9	21.1	44.5
E6	20	1.5 (1.9 wt%)	-	-	15.9	55.4	20.7	43.6
E7	20	2.0 (1.4 wt%)	-	-	20.4	59.0	22.4	47.3

^a determined on dry basis; ^b substrate to catalyst molar ratio: mol of anhydrous glucose unit in the starting biomass/mol of catalyst; ^c Glu = glucose; AA = acetic acid; FA = formic acid.

For both C and E samples, no significant decrease of the yields was observed increasing the biomass loading. On the other hand, higher LA concentrations, from 15.9 up to 34.6 g/L for C samples, and from 25.5 to 58.9 g/L for E ones, were reached. Considering that lower concentrations of HCl allow minimizing environmental impact and process costs, Table 2 reports the results of experiments performed with lower HCl amounts, increasing the substrate/catalyst ratios from 0.9 up to 2.0 mol/mol, run C5, C6, C7 and runs E5, E6 and E7, for C and E samples respectively. These runs evidenced that LA molar yield is not affected by the reduction of the catalyst content, at least in the range of the investigated substrate to catalyst ratios. For both C and E samples, promising values of LA molar yields were obtained, as well as no significant formation of side-products. In the case of E biomass hydrolysis, even acetic acid was not observed, due to the low content of acetyl groups in this feedstock. As expected, higher LA concentrations were

achieved from the cellulose-rich steam-exploded cardoon (E sample) rather than from that un-treated (C sample): the maximum reached value was 59.0 g/L for E and 34.6 g/L for C. On the other hand, it is interesting that the reactivity of the cellulosic fraction of the exploded biomass E is very similar to that of the untreated sample C, thus suggesting that pretreatment does not significantly modify the accessibility of the cellulose fibers. Regarding FA, its formation is almost equimolar with respect to LA for runs C3-E3 of Table 2, as expected from the overall hydrolysis reaction mechanism, whilst this correspondence does not fully fit for the remaining runs E4-E7 of Table 2 (lower FA molar concentration than the theoretical one), probably due to a combined effect of the type of feedstock, which has been previously steam-exploded (resulting more reactive than the crude sample to the hydrolysis), and of the high loading used for these runs, both leading to its more appreciable thermal degradation to CO₂ and H₂ in the liquid phase.

At the end of every run, a solid residue was recovered, accounting for about 30 wt% respect to the starting dry biomass. Due to the ponderal relevance of these residues, their characterization and applicative perspectives will be discussed later.

Regarding the presence of by-products, the reaction mixture certainly includes also low amounts of soluble impurities, which have not been considered up to now and which should be otherwise better characterized, to get information about the proper work-up procedures, although the concentration of any single by-product in the hydrolyzates is under the limit of detection of the HPLC analysis by routine refractive index detector (0.1 g/L) and, for this reason, not inserted in Tables 1 and 2. To detect trace amounts of impurities, higher sensitivity mass and/or UV detectors should be used. For this purpose, first of all, the crude hydrolysate obtained from run E7 of Table 2 was extracted by diethyl ether and the recovered extract was analyzed by the GC-MS technique. The analysis revealed the presence of oxygenated C5 compounds and of aromatics of lignin sources, such as guaiacol (2-methoxy phenol) and syringol (2,6-dimethoxy phenol) (see Figure S1, Supplementary Section). The dehydration of C5 and C6 carbohydrates causes the formation of furanic monomers and soluble precursors of solid humins [32]. On the other hand, the above phenolic derivatives show characteristic absorptions in the ultraviolet region, in particular at 284 nm, due to carbonyl $n \rightarrow \pi^*$ transitions [33], while stronger carbonyl $\pi \rightarrow \pi^*$ transitions occur at a lower wavelength, at about 205 nm. Based on these statements, the HPLC-UV analysis of the crude hydrolysate was carried out at 284 and 205 nm, thus better differentiating furanic impurities from other carbonyl species, such as aliphatic carboxylic acids. Regarding the UV-HPLC chromatogram at 284 nm (Figure S2, Supplementary Section), it shows the presence of many furanic/aromatic species, which elute after 20 minutes, whereas at 205 nm aliphatic carbonyl species prevail (Figure S3, Supplementary Section). To obtain more in-depth information, the crude liquor was analyzed by HPLC-MS and Total Ion Current (TIC) chromatogram related to all ions of all detected masses and UV chromatograms at 280, 250 nm and 205 nm are reported in the Supplementary Section, together with the chromatographic data of the main detected compounds including, where possible, the best matched chemical formula (Figure S4 and Table S1, respectively). At this level of investigation, given the high sensibility of this technique, TIC signal due to the crude hydrolysate is very complex, including besides LA (compound n° 17 of Table S1, Supplementary Section), which by far represents the main product of interest, as previously stated, but also many impurities. The cross-comparison with the GC-MS data confirms the presence of methoxyphenol and 2,6-dimethoxyphenol (compounds n° 36 and n° 38 of Table S1 of Supplementary Section, respectively), as aromatics of lignin source. To obtain further useful information for the following discussion, some typical compounds deriving from biomass hydrolysis have been sought [34], paying particular attention to some selected carboxylic acids of interest [35]. On this basis, after having excluded the contribution of the LA as the main component, Extracted Ion Chromatogram (XIC) of some typical organic acids deriving from biomass hydrolysis treatments, have been acquired (Figure S5/Table S2 and Figure S6/Table S3 of Supplementary Section), thus ascertaining the

presence, in low abundance, of many of these, such as tartaric, malic, succinic, lactic, butyric, itaconic, maleic, pyruvic, glutaric, adipic, 2-hydroxy-2-methylbutyric, gluconic and citric acid. In addition, 5-HMF is still present, as well as its dimeric/trimeric derivatives, as confirmed by the corresponding XIC processing (Figure S7, Supplementary Section). Instead, furfural, the furanic compound deriving from the acid-catalyzed conversion of the hemicellulose fraction, has not been found, thus indirectly confirming the effectiveness of the steam-explosion treatment, which has allowed the preliminary removal of this biomass component. Lastly, glucose has been identified only in traces (Figure S5/Table S2 of Supplementary Section), confirming the effectiveness of the acid-catalyzed conversion of the C6 fraction, as highly desired by our approach.

Steam-exploded cardoon E was selected for further studies regarding the effect of temperature on the hydrolysis reaction and Table 3 reports the results achieved at the lower temperature of 180°C and the upper one of 200°C, in comparison with the run at the temperature of 190°C previously used. The obtained results confirm that 190°C is the best temperature for the production of LA, as highlighted in the literature for the hydrothermal treatment of many lignocellulosic biomasses [13].

Table 3. Hydrolysis experiments on wet E cardoon sample, with different temperatures. Experimental conditions: reaction time = 20 min, sub/cat = 2.0 mol/mol, biomass loading = 20 wt% (on dry basis), HCl as catalyst (1.4 wt%), MW heating.

Run	Temperature (°C)	Products (g/L) ^a				LA ponderal yield (wt%)	LA molar yield (mol%)
		Glu	AA	FA	LA		
E8	180	-	-	19.4	46.4	18.6	39.8
E7	190	-	-	20.4	59.0	22.4	47.3
E9	200	-	-	13.8	48.0	19.2	41.2

^a Glu = glucose; AA = acetic acid; FA = formic acid.

Finally, the effect of the reaction time on LA formation was investigated (runs E7, E10 and E11, Figure 2). As reported in Figure 2, experiments were carried out on E sample at 20, 40 and 60 minutes of MW irradiation, under the same reaction conditions of temperature (190°C), catalyst (HCl, 1.4 wt%), substrate to catalyst molar ratio (2.0 mol/mol) and biomass loading (20 wt%).

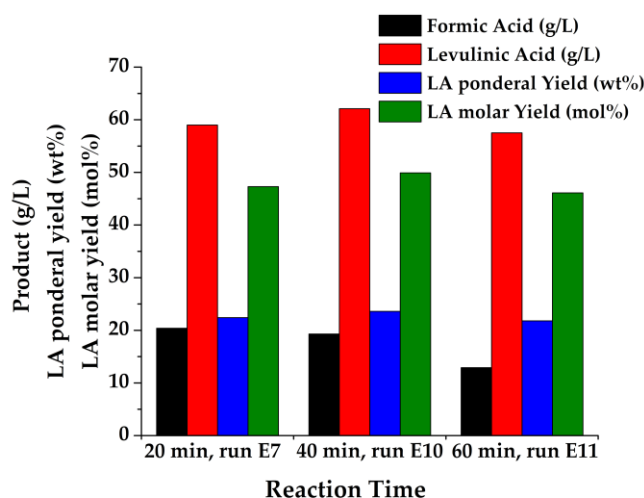


Figure 2. Hydrolysis experiments on wet E cardoon sample at different reaction times. Experimental conditions: 190°C, HCl as catalyst (1.4 wt%), sub/cat = 2.0 mol/mol, biomass loading = 20 wt% on dry basis, MW heating.

Only a weak time effect on the hydrolysis efficiency was observed, achieving the best LA yield of 49.9 mol% with the highest LA concentration of 62.1 g/L after 40 minutes of heating, adopting HCl in a low amount, 1.4 wt%.

2.3 Hydrolysis of *E cardoon* under conventional heating

Based on the results discussed in the previous section, cellulose-rich steam-exploded cardoon (E sample) resulted to be a particularly promising residual biomass for LA synthesis. Therefore, this hydrolysis reaction was also studied in a batch autoclave with conventional heating to verify the possible process intensification on an industrial scale. Taking into account that the heat transfer process in the autoclave is slower than the heating mechanism in the MW reactor, a longer reaction time (120 minutes) was applied in the autoclave, adopting two different biomass loading, 10 and 15 wt% on dry basis. For comparison, MW hydrolysis reactions had been carried out for 20 and 40 minutes, adopting the same biomass loadings. The results and the compositions of the main reaction products are reported in Table 4 and Figure 3, respectively.

Table 4. Hydrolysis experiments on wet E cardoon sample adopting different heating systems, biomass loadings and substrate to catalyst molar ratios. Experimental conditions: 190°C, HCl as catalyst.

Run	Biomass loading (wt%) ^a	sub/cat (mol/mol) ^b (HCl wt%)	Heating system	Time (min)	LA ponderal yield (wt%)	LA molar yield (mol%)
E3	10	0.9 (1.6 wt%)	MW	20	23.6	49.7
E12	10	0.9 (1.6 wt%)	autoclave	120	25.2	53.1
E13	15	1.5 (1.4 wt%)	MW	40	24.6	51.8
E14	15	1.5 (1.4 wt%)	autoclave	120	22.3	47.1

^a determined on dry basis; ^b substrate to catalyst molar ratio: mol of anhydrous glucose unit in the starting biomass/mol of catalyst.

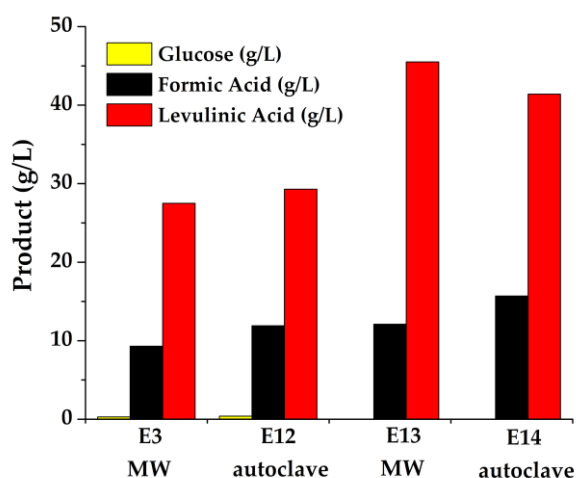


Figure 3. Compositions of the main reaction products of runs E3, E12, E13 and E14 reported in Table 3.

In the case of biomass loading of 10 wt%, similar LA molar yields were reached with the two heating systems, 49.7 and 53.1 mol% in MW and autoclave, respectively, while in the case of 15 wt% of biomass loading, heating in autoclave resulted in slightly lower yield, 47.1 mol%, compared to 51.8 mol% in MW, probably due to mass and heat transfer limitations. However, the comparable high LA concentrations reached both in the autoclave and in MW, 41.4 and 45.5 g/L respectively, demonstrate that both heating methodologies can be successfully applied for performing this process.

2.4 MW-assisted alcoholysis of *E cardoon* sample

In the second part of our investigation, the one-pot alcoholysis reaction of wet *E cardoon* in *n*-butanol to BL was studied in MW reactor and the results are reported in Table 5. The presence of a significant amount of introduced water, due to the high humidity of the sample, is an unprecedented approach respect to the up to now reported alcoholysis studies, performed in presence of alcohol alone as reactant/reaction medium. This procedure allowed us to convert efficiently the starting biomass, without the initial drying step, thus at the same time-saving time and significant resources.

Table 5. Butanolysis experiments on wet *E cardoon* sample, adopting different biomass loadings and catalyst amounts. Experimental conditions: 190°C, H₂SO₄ as catalyst, MW heating.

Run	Biomass loading (wt%) ^a	sub/cat (mol/mol) ^b (H ₂ SO ₄ wt%)	Time (min)	BL (g/L)	BL ponderal yield (wt%)	BL molar yield (mol%)
AE1	8	2.4 (1.3 wt%)	15	27.5	26.4	42.5
AE2	15	2.4 (2.4 wt%)	15	44.2	15.3	22.1
AE3	15	4.7 (1.3 wt%)	15	37.9	12.8	19.8
AE4	8	2.4 (1.3 wt%)	30	22.0	25.3	36.6
AE5	8	2.4 (1.3 wt%)	45	20.9	24.2	35.1

^a determined on dry basis; ^b substrate to catalyst molar ratio: mol of anhydrous glucose unit in the starting biomass/mol of catalyst.

In the presence of low contents of the acid catalyst H₂SO₄ (1.3 and 2.4 wt%) with the same substrate to catalyst molar ratio, and applying only 15 minutes of heating, the butanolysis led to BL molar yields of 42.5 and 22.1 mol%, using respectively the biomass loading of 8 and 15 wt% on dry basis, runs AE1 and AE2 (Table 5). When the lower catalyst loading of 1.3 wt% was maintained with the biomass loading of 15 wt%, a significant decrease of BL yield (19.8 mol%) was ascertained, essentially due to the above-mentioned mass transfer issues. Taking into account that the best BL yield, as well as a good BL concentration (27.5 g/L), were obtained in the run AE1, the effect of duration was studied adopting the same conditions but prolonging the reaction time to 30 and 45 minutes (runs AE4 and AE5, respectively). The achieved results show that the prolonging of the reaction time does not improve the BL production, whereas slightly lower BL yields and BL concentrations were obtained, demonstrating the efficacy of MW irradiation within a short reaction time. Finally, to better evaluate the impact of introduced water on the ascertained performances, an explorative run adopting the dry *cardoon E* sample was performed employing the same reaction conditions of run AE1: in this case,

the BL concentration of 17.9 g/L was achieved with BL ponderal and molar yields of 26.4 wt% and 38.3 mol% respectively, resulting similar to that ascertained on wet cardoon. In all the above runs only traces of levulinic acid were detected, thus confirming that under an excess of bio-alcohol the hydrolysis reaction is irrelevant, also when a certain of humidity is introduced with the wet biomass.

At the end of the reaction for every run, a significant amount of solid residue was also ascertained, whose characterization and potential valorization will be discussed below.

The results of this preliminary study demonstrate that direct BL production can be performed not only from conventional starting materials (LA, disaccharides, polysaccharides and furfuryl alcohol [22]) but also directly, using raw steam-exploded defatted cardoon as the starting feedstock, opening the way to the direct conversion of the cellulosic fraction of this cheap, residual biomass in a valuable intermediate/bio-fuel.

2.5 Characterization of post-reaction solid residues

The solid residues recovered from the best MW-assisted hydrolysis and alcoholysis reactions to LA and BL, runs E7 and C7 for hydrolysis and run AE1 for alcoholysis, amounted respectively 30.6, 31.4 and 27.4 wt% of the starting biomass, calculated on dry basis. All these samples were analyzed by elemental analysis and Table 6 reports the obtained results, compared with the C and E dry cardoon samples starting feedstocks.

Table 6. Results of the elemental analysis for the starting C and E dry cardoon samples, for the solid residues at the end of runs C7 and E7 (hydrolysis reactions) and for the solid residue at the end of run AE1 (alcoholysis reaction).

Sample	C (%)	H (%)	N (%)	S (%)	O (%) ^a	Ash (%)	H/C	O/C	HHV (MJ/kg)
Cardoon C – starting feedstock	43.5	6.4	0.2	0.3	49.6	7.2	1.8	0.9	17.47
Cardoon E – starting feedstock	47.8	6.4	0.2	0.2	45.4	0.0	1.6	0.7	19.57
Solid residue, run C7	66.9	5.1	0.1	0.1	27.8	0.2	0.9	0.3	26.49
Solid residue, run E7	66.4	5.2	0.1	0.1	28.2	0.3	0.9	0.3	26.39
Solid residue, run AE1	65.3	5.2	0.2	0.1	29.2	0.3	0.9	0.3	25.90

^aOxygen content was calculated by difference: O (%) = 100 (%) – C (%) – H (%) – N(%) – S(%).

The above data related to the starting feedstocks confirm a limited beginning of carbonization, as shown by the increase in carbon content, occurred as a consequence of the mild steam-explosion treatment, aimed at the breakdown of the biomass matrix (cross-linking lignin), the bulk solubilization of the hemicellulose fraction and the removal of smaller hydrocarbon molecules (volatiles and gases) [36]. Instead, more advanced carbonization has occurred as a consequence of the acid-catalyzed hydrothermal treatment. H/C and O/C molar ratios of both solid residues at the end of runs C7 and E7 fall within the range reported in the literature for the hydrochars (H/C: ~0.8–1.4 and O/C: ~0.3–0.5) [37] and also in agreement with our previous work [38]. Therefore, the differences in the carbon content of the two different starting feedstocks have been attenuated by the acid-catalyzed hydrothermal treatment, demonstrating the complete carbonization occurred with this technology. Lastly, the post-alcoholysis residue does not show significant compositional differences respect to the post-hydrolysis ones, thus highlighting the similarity between the performed hydrolysis/alcoholysis treatments. These conclusions are also evident from the Van Krevelen diagram shown in Figure 4 which plots the molar ratios of the H/C and O/C for both the starting biomasses, cardoon sam-

ples C and E, and for the solid residues at the end of runs C7 and E7 for hydrolysis and run AE1 for butanolysis.

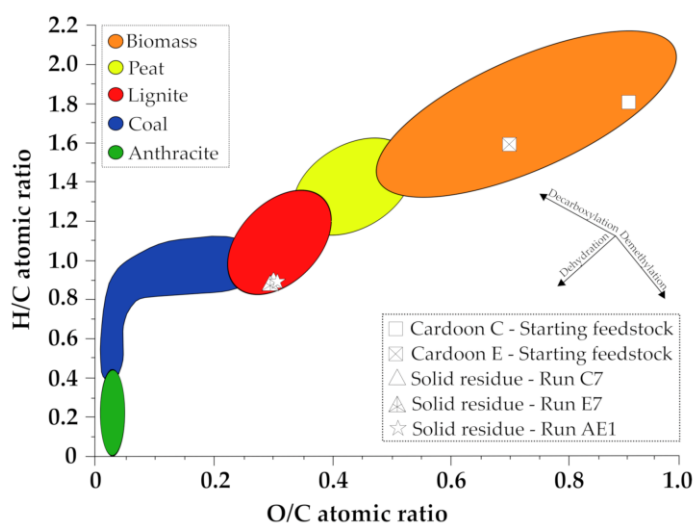


Figure 4: Van Krevelen diagram of starting biomasses, cardoon sample C7 and E7, and solid residues at the end of runs C7 and E7 for alcoholysis and run AE1 for butanolysis.

The positions of the starting feedstocks and the corresponding chars in the Van Krevelen diagram confirm that, in all cases, dehydration is the main allowed path, leading to the formation of carbonaceous material and the H/C and O/C ratios of all the obtained residues fall within the range reported in the literature for this kind of biomaterials (H/C: ~0.8–1.4 and O/C: ~0.3–0.5) [38,39]. In addition, the higher heating value (HHV) was calculated from elemental analysis (Table 6): the ascertained values significantly increase going from the starting feedstock to the corresponding chars, thus resulting comparable with that of the traditional lignite coal, in agreement with the conclusions gathered from the Van Krevelen plot [39].

Furthermore, FT-IR characterization of the post-reaction solid residues was performed and Figure 5 shows the FT-IR spectra registered in ATR mode both for the starting crude cardoon, both C and E samples, and for the solid residues recovered after hydrolysis reactions, runs E7 and C7.

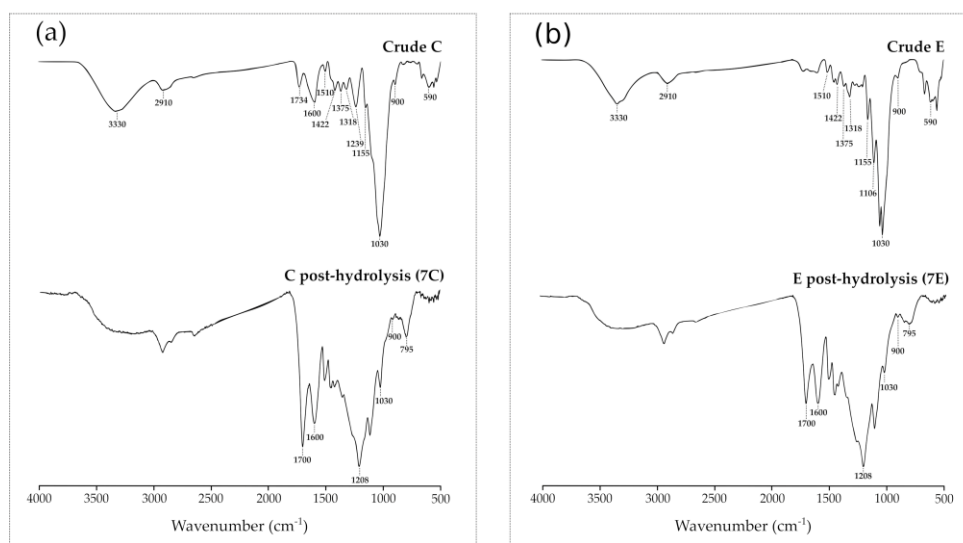


Figure 5. FT-IR spectra registered in ATR mode for the starting crude cardoon, both C and E samples, and for the solid residues recovered after hydrolysis reactions, runs E7 and C7.

The spectrum of crude sample C shown in Figure 5(a) shows characteristic signals of the three bio-polymers, cellulose, hemicellulose and lignin: a broad band at about 3330 cm^{-1} assigned to vibration mode of O-H bonds and a band at 2910 cm^{-1} assigned to C-H stretching of methyl and methylene groups. The peak at 1734 cm^{-1} is due to C=O stretching in the acetyl group and carboxylic acid of hemicellulose, while the signals at 1600 and 1510 cm^{-1} are attributed to aromatic C=O stretching and C=C vibration of lignin [39,40]. Weak peaks are observed at 1422, 1375 and 1318 cm^{-1} that can be assigned to the C-H asymmetric mode of CH_2 in cellulose, aromatic C-H and C-O in lignin, respectively [41, 42]. The band at 1239 cm^{-1} is due to the C-O stretching of alcoholic, phenolic and ether groups [42]. The peak at 1155 cm^{-1} is assigned to C-O-C asymmetric stretching in cellulose and hemicellulose, the intense peak at 1030 cm^{-1} to C-O-H stretching and the one at 900 cm^{-1} to anomeric vibration at the β -glycosidic linkage, while the band at 590 cm^{-1} can be due to aromatic C-H bonds [38,43]. As expected, the peaks at 1734 and 1600 cm^{-1} are not noticeable in the spectrum of crude sample E showed in Figure 5(b), since the steam-explosion pre-treatment degrades hemicellulose and lignin. The FT-IR spectroscopy in ATR mode allows the characterization of functional groups on the material surface and the analysis is in agreement with the bulk composition determined by the NREL procedure for the samples of raw cardoon. In the case of the solid residues recovered after the post-hydrolysis reactions 7E and 7C, reported again in Figure 5(a) and 5(b) respectively, peaks characteristic of cellulose, such as the intense peak at about 1030 cm^{-1} and the peak at about 900 cm^{-1} , are strongly decreased in accordance with the fact that cellulose was efficiently converted to LA. However, signals that may be assigned to by-products, such as humins, appear: a peak at about 1700 cm^{-1} due to the C=O stretching, another one at about 1600 cm^{-1} due to stretching vibration of C=C bonds of furanic rings and the last one at about 795 cm^{-1} due to aromatic bending off the plane of the C-H bond [38,44] are evident in the spectrum of both post-hydrolysis residues. Broad absorbance in the 1300–1100 cm^{-1} region could be ascribed to multiple C–OH stretching bonds. However, the intense signal at 1208 cm^{-1} evident in the post-hydrolysis residues 7C and 7E could arise also from the presence of ether bonds [44]. Humins can result from condensation reactions between sugars, HMF and intermediates during the dehydration of carbohydrates [45–48] and their formation can be competitive with the re-hydration of HMF to LA. Moreover, humins are complex and recalcitrant carbonaceous materials that can cover the substrate surface, making it less accessible to acid attack.

Figure 6 reports the FT-IR spectra of the solid residue recovered after the butanolysis reaction AE1 together with again the starting crude E sample.

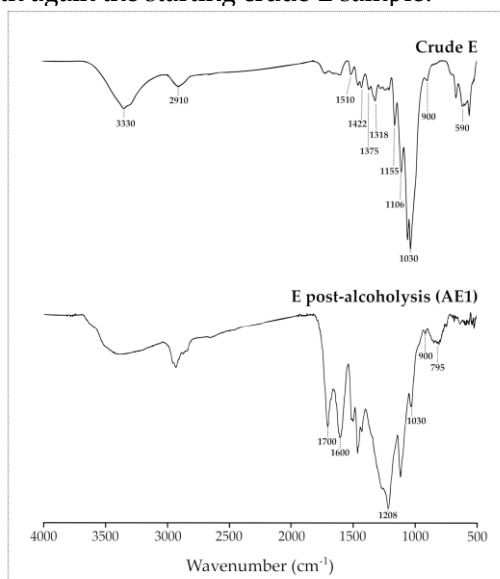


Figure 6. FT-IR spectra registered in ATR mode for the starting cardoon E sample and that of the solid residue recovered after alcoholysis reaction AE1.

In Figure 6, the FT-IR spectrum of the post-alcoholysis char is shown, resulting very similar to that obtained after hydrothermal processing (Figure 5). In particular, the absorption bands at 1700 and 1600 cm^{-1} (C=O and C=C stretching vibrations, respectively) are visible also in the post-alcoholysis char, as well as that at 1030 cm^{-1} (C-O-H stretching in cellulose), even if in this case of lower intensity respect to the crude E feedstock, thus confirming the occurred cellulose decomposition, as previously stated. In addition, the absorption bands at 1208 cm^{-1} (C-O stretching), and 795 cm^{-1} (C-H bending off the plane) further confirm the similarity between the chars produced by hydrolysis/alcoholysis. At this stage of the investigation, the severity of the performed treatments dampens any differences deriving from the use of different reaction solvents, otherwise reported by some authors very recently [49].

Moreover, the recovered residues and the starting biomasses were also characterized by thermogravimetric analysis and weight loss and weight loss thermograms are depicted in Figure 7.

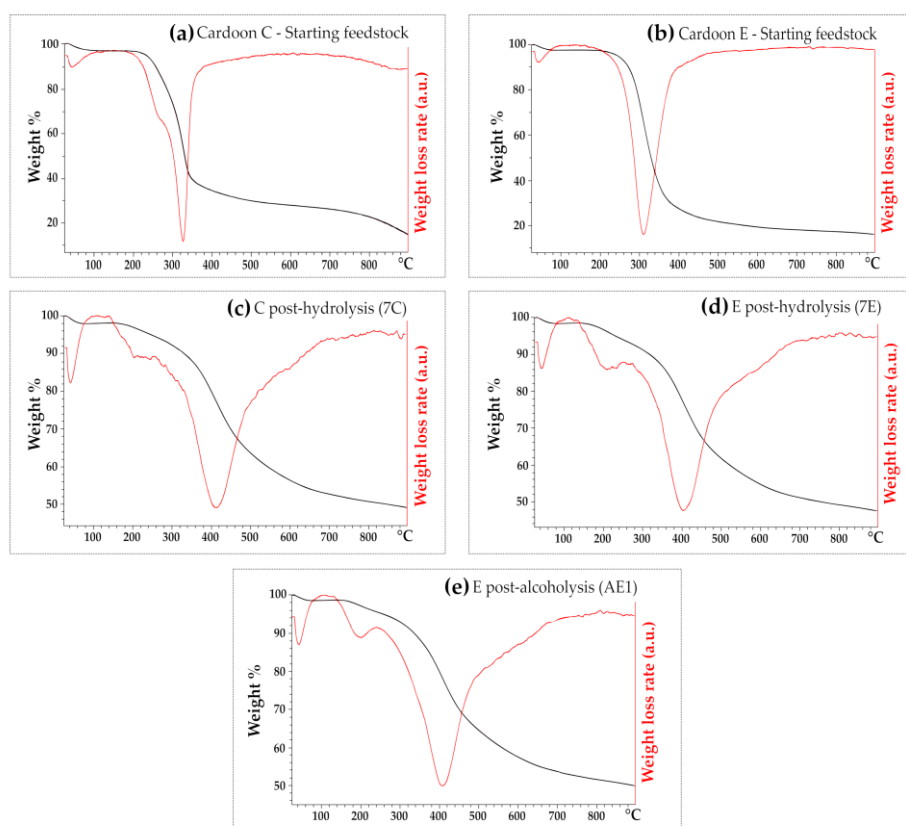


Figure 7. TGA analysis of the starting crude cardoon, both C and E samples (a and b), of the solid residues recovered after hydrolysis reactions, runs C7 and E7 (c and d) and of the solid residue recovered after alcoholysis reaction AE1 (e): weight loss (black line) and weight loss rate (red line).

Regarding the devolatilization behavior of the starting feedstocks (Figure 7, thermograms (a) and (b)), the first peak is found below 100 $^{\circ}\text{C}$ and is due to the loss of humidity. The degradation of the cardoon starts at higher temperatures, in particular, a shoulder is found at about 250 $^{\circ}\text{C}$, present only in the C cardoon starting feedstock, ascribed to hemicellulose fraction, overlapped with that of cellulose, in the range 300-350 $^{\circ}\text{C}$ [50,51]. Lastly, lignin degradation is very slow, occurring for the whole temperature range of the thermogravimetric analysis [50]. The comparison between the thermograms of the starting feedstocks, C and E cardoon samples ((a) and (b)), confirms the effectiveness of the steam-explosion treatment, which has allowed the selective removal of the hemicellulose fraction. Moreover, the E cardoon starting feedstock shows a

very weak shoulder at about 400 °C, which is due to the lignin component [50], which resulted more accessible and reactive as a consequence of the occurred steam-explosion pre-treatment. On the other hand, the three residues deriving from hydrolysis/alcoholysis treatments ((c), (d), (e)) show analogous thermal profiles, thus confirming their chemical similarity, also in agreement with the previous characterization data. Again, the humidity loss of these samples occurs below 100 °C, then a degradation step was found at about 200 °C, due to the release of some organic compounds (such as LA and FA), trapped into this porous bio-material [52]. The absence of the degradation steps of hemicellulose and cellulose fractions confirms the effectiveness of the performed hydrolysis/alcoholysis treatments, whereas the main peak at about 400 °C is attributed to the decomposition of volatile lignin/furanic structures [52,53]. In all cases of the synthesized residues, a final weight loss of ~50 wt% was ascertained, thus revealing increased thermal stability than the starting biomass and demonstrating the occurred similar carbonization [38], also in agreement with the previous characterization data.

The characterization of the obtained solid residues opens the way to their uses. Regarding this aspect, certainly the most immediate use is the combustion for the energy recovery, but this choice is currently considered as the last option, preferring, when possible, its reuse within the scopes of the circular economy [54]. For agricultural uses, the application of biochar to the soil can mitigate climate change by promoting carbon sequestration and decrease greenhouse gas emissions [55]. Moreover, char has been advantageously proposed as a growing medium, to be used in combination with other components (vermiculite, clays, etc.) to improve physicochemical soil properties, such as increase in cation exchange capacity, water holding capacity, available water, improvement of soil structure, reduction in soil acidity, microbiological activity, quality, and yield of the crops [55]. Use of the char as a soil amendment for the recovery of contaminated soils, including stabilization of organic and inorganic contaminants, has been proposed and seems attractive [55]. Lately, more added-value char-based products are under development in many research fields, such as adsorption, catalysis and electrochemical energy storage (lithium-ion batteries, lithium-sulfur batteries, sodium-ion batteries and supercapacitors), after having properly tuned its porosity and functional groups, by choosing the appropriate starting feedstocks and optimizing the reaction conditions [56].

3. Materials and Methods

3.1 Materials

Two types of cardoon waste residues after seeds removal were investigated: non pre-treated cardoon (C) and steam-explosion pre-treated one (E). Catalysts and chemicals were purchased from Sigma-Aldrich and employed as received: hydrochloric acid (HCl, 37 wt%), sulfuric acid (H₂SO₄, 95 wt%), 5-hydroxymethyl-2-furaldehyde (HMF, 98%), levulinic acid (LA, 98%), formic acid (FA, 98%), glucose (Glu, 99.5%), acetic acid (AA., 99%), furfural (99%), diethyl ether (98%), water for HPLC; *n*-butanol (94,5%), *n*-dodecane (99%), *n*-butyl levulinate (BL, 98%). Both C and E cardoon samples were used as received and/or after a drying step carried out at 105 °C in an oven until a constant weight was reached.

The biomass loading and the catalyst amount were calculated according to the following equations, respectively:

$$\text{Biomass loading (wt\%)} = \frac{\text{employed dry biomass (g)}}{[\text{employed biomass (for dry or wet samples) (g)} + \text{solvent (g)}]} \times 100;$$
$$\text{Catalyst (wt\%)} = \frac{\text{catalyst (g)}}{[\text{catalyst (g)} + \text{employed biomass (for dry or wet samples) (g)} + \text{solvent (g)}]} \times 100.$$

3.2 Steam-explosion process conditions

The steam-explosion pretreatment has been carried out on the untreated *Cynara cardunculus* L. sample C using the CRB/CIRIAF equipment [28]. In particular, 447.50 g of dry cardoon sample was treated at 165°C and 200 bar for 10 minutes, employing the severity factor Log R0 equal to 2.91.

3.3 Compositional analysis of raw biomass

For both C and E cardoon residues, the contents of cellulose, hemicellulose and lignin were determined according to the NREL protocol, as well as extractives and ash [57]. Also the content of humidity was estimated according to the NREL procedure [58].

3.4 Acid-catalyzed hydrolysis of cardoon

Hydrolysis reactions were carried out in deionized water, using HCl or H₂SO₄ as catalyst, in the single-mode MW reactor CEM Discover S-class System (maximum pulsed-power 300 W, 35 mL pyrex vial). The reaction slurries were mixed with a magnetic stirrer and irradiated up to the set-point temperature for the selected reaction time. During the reaction, pressure and temperature values were continuously acquired with the software and controlled with a feedback algorithm to maintain the constant temperature. Batch experiments were carried out also in an electrically heated 600 mL Parr zirconium made-fixed head autoclave equipped with a P.I.D. controller (4848). The reactor was pressurized with nitrogen up to 30 bar and the reaction mixtures were stirred using a mechanical overhead stirrer. The reactions were carried out at the selected temperature for the chosen time. At the end of each reaction, the reactors were rapidly cooled at room temperature by blown air, the hydrolyze was separated from solid residuals by vacuum filtration, filtered with a PTFE filter (0.2 µm) and analyzed through high-pressure liquid chromatography (HPLC) with a refractive index detector.

3.5 Acid-catalyzed alcoholysis of cardoon

Alcoholysis reactions were carried out in *n*-butanol, using H₂SO₄ as catalyst, in the MW reactor CEM Discover S-class System at 190°C for the selected reaction time. At the end of each reaction, the slurry was filtered under vacuum on a crucible and the liquid samples were diluted with acetone and analyzed by a gas chromatograph coupled with a flame ionization detector (GC-FID).

3.6 Analytical techniques

Liquid samples deriving from hydrolysis were analyzed by an HPLC system (Perkin Elmer Flexer Isocratic Platform) equipped with a Benson 2000-0 BP-OA column (300 mm x 7.8 mm) and coupled with a Waters 2140 refractive index detector. A 0.005 M H₂SO₄ aqueous solution was adopted as mobile phase, maintaining the column at 60 °C with the flow-rate of 0.6 mL/min. The concentrations of hydrolysis products were determined from calibration curves obtained with external standard solutions. Each analysis was carried out in duplicate and the reproducibility of this analysis was within 3%.

Liquid samples from alcoholysis were analyzed by a GC-FID instrument (DANI GC1000 DPC) equipped with a fused silica capillary column – HP-PONA cross-linked methyl silicone gum (20 m x 0.2 mm x 0.5 µm). The injection and flame ionization detector ports were set at 250°C. The oven temperature program was set at 90°C for 3 minutes and then increased at the rate of 10°C/min till it reached 260°C, where it was maintained for 5 minutes and up to 280°C with the rate of 10 °C/min and maintained for 3 minutes. Nitrogen was used as the carrier gas, at the flow rate of 0.2 mL/min. The quantitative analysis of alcoholysis products was performed by calibration using *n*-dodecane as internal standard. Each analysis was carried out in duplicate and the reproducibility of this analysis was within 5%.

The molar and the ponderal yields of the compounds of interest were calculated according to the following equations, respectively:

$$\text{Molar Yield (mol\%)} = [\text{product (mol)}/\text{anhydrous glucose unit in starting biomass (mol)}] \times 100;$$
$$\text{Ponderal Yield (wt\%)} = [\text{product (g)}/\text{dry starting biomass (g)}] \times 100.$$

Analysis of impurities was performed by GC-MS and HPLC-MS. When GC-MS analysis was carried out, the starting aqueous hydrolysate was extracted with diethyl ether and the diluted extract (about 0.1–0.2 μL) was qualitatively analyzed by the instrument Hewlett-Packard HP 7890 (Palo Alto, CA, USA), equipped with an MSDHP 5977 detector and with a G.C. column Phenomenex Zebron with a 100% methyl polysiloxane stationary phase (column length 30 m, inner diameter 0.25 mm and thickness of the stationary phase 0.25 μm), in splitless mode. The transport gas was helium 5.5 and the flow was 1 mL/min. The temperature of the injection port was set at 250 $^{\circ}\text{C}$, carrier pressure at 100 kPa. The oven was heated at 50 $^{\circ}\text{C}$ for 1 minute, then the temperature was raised at 3 $^{\circ}\text{C}/\text{min}$ up to 250 $^{\circ}\text{C}$ and held for 5 minutes. When HPLC-MS analysis was carried out, a Sciex X500 qTOF mass spectrometer (Sciex, Darmstadt, Germany) was coupled to an HPLC Agilent 1260 Infinity II (Agilent, Waldbronn, Germany) and operated in ESI negative mode (spray voltage of -4500 V). HPLC system was equipped with a diode-array detector (DAD), which operated at 210, 250 and 280 nm. Chromatographic separation was achieved on a Zorbax SB-C18 column 150 mm \times 4.6 mm, particle size 3.5 μm (Agilent, California, United States) as the stationary phase, using water with 0.1% (v/v) of formic acid (A) and methanol (B) as the eluents. The mobile phase flow rate was 0.7 mL/min, and the column oven temperature was set at 25 $^{\circ}\text{C}$. The gradient was programmed as follows: 0–22.0 min at 95% (A), 22.0–30.0 min at 5% (A), 30.0 min at 95% (A), held for 5 min. The sample was filtered and 10 μL were injected into the HPLC system, after proper dilution (1:1) and filtration.

Fourier Transform-Infrared (FT-IR) spectra for raw biomasses and solid residues after reactions were recorded in attenuated total reflection (ATR) mode with a Spectrum-Two Perkin-Elmer spectrophotometer. The acquisition of each spectrum provided 12 scans, with a resolution of 8 cm^{-1} , in the wavenumber range between 4000 and 450 cm^{-1} .

Thermogravimetric analysis (TGA) of starting feedstocks and solid residues after reactions was performed with a Mettler Toledo TGA/SDTA 851 apparatus in high purity N_2 . The sample was heated from 30 $^{\circ}\text{C}$ up to 900 $^{\circ}\text{C}$, at a rate of 10 $^{\circ}\text{C}/\text{min}$, under nitrogen atmosphere (60 mL/min). Both weight loss and weight loss rate were acquired during each experiment.

Elemental analysis (C, H, N, S) of starting feedstocks and solid residues after reactions was performed by a commercially available automatic analyzer Elementar Vario MICRO Cube (Elementar, Germany). These elements were quantified adopting a thermal conductivity detector (TCD). Lastly, oxygen content was calculated by difference: $\text{O (\%)} = 100 (\%) - \text{C (\%)} - \text{H (\%)} - \text{N (\%)} - \text{S (\%)}$. HHV was calculated according to the following correlation proposed by Channiwala and Parikh [59]:

$$\text{HHV (MJ/Kg)} = 0.3491 \text{ C(\%)} + 1.1783 \text{ H(\%)} + 0.1005 \text{ S(\%)} - 0.1034 \text{ O(\%)} - 0.0151 \text{ N (\%)} - 0.0211 \text{ Ash(\%)}.$$

4. Conclusions

In this paper, the acid-catalyzed hydrolysis and alcoholysis of waste cardoon residues from the agro-industry to give strategic platforms LA and BL, respectively, were investigated. After removal of oil seeds, the cardoon was employed directly and after a steam-explosion pre-treatment, this last affording a cellulose-rich feedstock. This positive

effect of the SE pretreatment can be applied to a larger scale only if its economic sustainability is verified: in this sense a specific cost-benefit analysis should be developed case by case, considering that the more expensive sub-section of the SE facility is the vapor generator.

MW-assisted hydrolysis reactions on this last biomass led to high values of LA molar yield and concentration, up to 49.9 mol% and 62.1 g/L, respectively. The hydrolysis was also performed in a traditional batch autoclave, reaching LA yield and concentration of 47.1 mol% and 41.4 g/L, respectively, demonstrating that such process can be successfully intensified, by switching to traditional industrial reactors. The achieved results are really interesting, highlighting that eco-friendly reaction conditions, such as high biomass to acid catalyst ratio, water as the reactant/reaction medium and energy-saving heating, can be adopted for the conversion of low-cost residual cardoon, implying that sustainable exploitation of such biomass can be developed. Moreover, a preliminary study on the acid-catalyzed butanolysis of steam-exploded cardoon led to good BL yields, up to 42.5 mol%, proving that the direct one-pot conversion of the cellulosic fraction of this waste biomass can supply a wider range of value-added products, including bio-fuels. Moreover, the characterization of the solid residues recovered from both processes has allowed us to envisage their possible exploitation, in a perspective of the complete valorization of cardoon biomass.

The proposed approaches represent alternative solutions to reduce consumption of fossil resources and carbon dioxide emission and recycle massive amounts of agricultural residues, in agreement with the concept of third-generation biorefinery.

Supplementary Materials: The following are available online at www.mdpi.com/xxx/s1, Figure S1: Total ion chromatogram (TIC) of the diethyl ether extract and corresponding mass spectra of the identified compounds, Figure S2: RI-and UV-HPLC chromatogram of the crude hydrolysate at 284 nm, Figure S3: UV-HPLC chromatograms of the crude hydrolysate at 205 and 284 nm, Figure S4: TIC related to all ions of all detected masses and corresponding UV chromatograms (280, 250 nm, superimposed) and 205 nm, Figure S5: XIC chromatogram obtained from selected compounds of interest, according to Glińska et al. For numbering and corresponding assignments, see Table S2, Figure S6: XIC chromatogram obtained from selected compounds of interest, according to Ibáñez et al. For numbering and corresponding assignments, see Table S3, Figure S7: Monomeric/oligomeric (as dimeric/trimeric) compounds of 5-HMF and corresponding XIC chromatogram, Table S1: Chromatographic data of the main detected compounds reported in Figure S4, Table S2: Chromatographic data of selected compounds of interest for hydrolyzates of biomass source, according to Glińska et al. (see also XIC chromatogram of Figure S5), Table S3: Chromatographic data of selected compounds of interest for hydrolyzates of biomass source, according to Ibáñez et al. (see also XIC chromatogram of Figure S6).

Author Contributions: A.M.R.G., C.A., S.C., and D.L. conceived the experiments; A.M.R.G., S.C., D.L. N.D.F. and C.A. designed the experiments; N.D.F., S.C., V.C. and D.L. performed the experiments and analysis; all the authors analysed the data; A.M.R.G., C.A., S.C., V.C. and D.L. wrote the paper; N.D.F. and F.C. revised and supervised the writing of the manuscript. All authors have read and agreed to the published version of the manuscript.

Funding: This research was funded by the project VISION PRIN 2017 FWC3WC_002 funded by MIUR and by the project PRA_2018_26 funded by University of Pisa.

Acknowledgments: The project VISION PRIN 2017 FWC3WC_002 and the project PRA_2018_26 of University of Pisa are gratefully acknowledged.

Conflicts of Interest: The authors declare no conflict of interest. The funders had no role in the design of the study; in the collection, analyses, or interpretation of data; in the writing of the manuscript, or in the decision to publish the results.

1. Puricelli, S.; Cardellini, G.; Casadei, S.; Faedo, D.; Van den Oever, A.E.M.; Grosso, M. A review on biofuels for light-duty vehicles in Europe. *Renew. Sust. Energ. Rev.* **2021**, *137*, 110398. doi.org/10.1016/j.rser.2020.110398. 714-715
2. Falcone, P.M.; Lopolito, A.; Sica, E. The networking dynamics of the Italian biofuel industry in time of crisis: Finding an effective instrument mix for fostering a sustainable energy transition. *Energy Policy* **2018**, *112*, 334–348. doi.org/10.1016/j.enpol.2017.10.036. 716-718
3. Greenhouse Gas Emissions, US EPA. Available online: <https://www.epa.gov/ghgemissions/overview-greenhouse-gases> (accessed on 29 June 2021). 719-720
4. IPCC, 2014: Climate Change 2014: Synthesis Report. Contribution of Working Groups I, II and III to the Fifth Assessment Report of the Intergovernmental Panel on Climate Change. Core Writing Team, R.K. Pachauri and L.A. Meyer, Eds. IPCC, Geneva, Switzerland, 151 pp. 721-723
5. Coccia, V.; Cotana, F.; Cavalaglio, G.; Gelosia, M.; Petrozzi, A. Cellulose Nanocrystals Obtained from *Cynara cardunculus* and Their Application in the Paper Industry. *Sustainability* **2014**, *6*, 5252–5264. doi.org/10.3390/su6085252. 724-725
6. Barracosa, P.; Barracosa, M.; Pires, E. Cardoon as a Sustainable Crop for Biomass and Bioactive Compounds Production. *Chem. Biodivers.* **2019**, *16*, e1900498. doi.org/10.1002/cbdv.201900498. 726-727
7. Zayed, A.; Serag, A.; Farag, M.A. *Cynara cardunculus* L.: Outgoing and potential trends of phytochemical, industrial, nutritive and medicinal merits. *J. Funct. Foods* **2020**, *69*, 103937. doi.org/10.1016/j.jff.2020.103937. 728-729
8. Grammelis, P.; Malliopoulou, A.; Basina, P.; Danalatos, N.G. Cultivation and Characterization of *Cynara cardunculus* for Solid Biofuels Production in the Mediterranean Region. *Int. J. Mol. Sci.* **2008**, *9*, 1241–1258. doi.org/10.3390/ijms9071241. 730-731
9. Fernández, J.; Curt, M.D.; Aguado, P.L. Industrial applications of *Cynara cardunculus* L. for energy and other uses. *Ind. Crops Prod.* **2006**, *24*, 222–229. doi: 10.1016/j.indcrop.2006.06.010. 732-733
10. Espada, J.J.; Villalobos, H.; Rodríguez, R. Environmental assessment of different technologies for bioethanol production from *Cynara cardunculus*: A Life Cycle Assessment study. *Biomass Bioenergy* **2021**, *144*, 105910. doi.org/10.1016/j.biombioe.2020.105910. 734-736
11. Sun, Y.; Cheng, J. Hydrolysis of lignocellulosic materials for ethanol production: a review. *Bioresour. Technol.* **2002**, *83*, 1–11. [https://doi.org/10.1016/S0960-8524\(01\)00212-7](https://doi.org/10.1016/S0960-8524(01)00212-7). 737-738
12. Overend, R.P.; Chornet, E. Fractionation of lignocellulosics by steam-aqueous pretreatments. *Philos. Trans. A Math. Phys. Sci. Series A: Mathematical and Physical Sciences* **1987**, *321*, 523–536. doi.org/10.1098/rsta.1987.0029. 739-740
13. Antonetti, C.; Licursi, D.; Fulignati, S.; Valentini, G.; Raspolli Galletti, A.M. New Frontiers in the Catalytic Synthesis of Levulinic Acid: From Sugars to Raw and Waste Biomass as Starting Feedstock. *Catalysts* **2016**, *6*, 196–225. doi.org/10.3390/catal6120196. 741-743
14. Bozell, J.J.; Petersen, G.R. Technology development for the production of bio-based products from biorefinery carbohydrates: The U.S. Department of Energy's "Top 10" revisited. *Green Chem.* **2010**, *12*, 539–554. doi: 10.1039/B922014C. 744-745
15. Leal Silva, J.F.; Grekin, R.; Pinto Mariano, A.; Maciel Filho, R. Making levulinic acid and ethyl levulinate economically viable: a worldwide techno-economic and environmental assessment of possible routes. *Energy Technol.* **2018**, *6*, 613–639. doi.org/10.1002/ente.201700594. 746-748
16. Christensen, E.; Williams, A.; Paul, S.; Burton, S.; McCormick, R.L. Properties and performance of levulinate esters as diesel blend components. *Energ. Fuels* **2011**, *25*, 5422–5428. doi.org/10.1021/ef201229j. 749-750
17. Howard M.S.; Issayev, G.; Naser, N.; Sarathy, S.M.; Farooq, A.; Dooley, S. Ethanolic gasoline, a lignocellulosic advanced biofuel. *Sustain. Energ. Fuels* **2019**, *3*, 409–421. doi.org/10.1039/C8SE00378E. 751-752
18. Licursi, D.; Antonetti, C.; Fulignati, S.; Giannoni, M.; Galletti Raspolli, A.M. Cascade strategy for the tunable catalytic valorization of levulinic acid and γ -valerolactone to 2-methyltetrahydrofuran and alcohols. *Catalysts* **2018**, *8*, 277–292. doi.org/10.3390/catal8070277. 753-755
19. Rivas, S.; Raspolli Galletti, A.M.; Antonetti, C.; Licursi, D.; Santos, V.; Parajó, J.C. A biorefinery cascade conversion of hemicellulose-free *Eucalyptus Globulus* wood: Production of concentrated levulinic acid solutions for γ -valerolactone sustainable preparation. *Catalysts* **2018**, *8*, 169–184. doi.org/10.3390/catal8040169. 756-758
20. Rackemann, D.W.; Doherty, W.O. The conversion of lignocellulosics to levulinic acid. *Biofuel. Bioprod. Biorefin.* **2011**, *5*, 198–214. doi.org/10.1002/bbb.267. 759-760
21. Timokhin, B.V.; Baransky, V.A.; Eliseeva, G.D. Levulinic acid in organic synthesis. *Russ. Chem. Rev.* **1999**, *68*, 73–84. doi.org/10.1070/RC1999v068n01ABEH000381. 761-762
22. Démolis, A.; Essayem, N.; Rataboul, F. Synthesis and Applications of Alkyl Levulinates. *ACS Sustain. Chem. Eng.* **2014**, *2*, 1338–1352. doi.org/10.1021/sc500082n. 763-764
23. Hishikawa, Y.; Yamaguchi, M.; Kubo, S.; Yamada, T. Direct preparation of butyl levulinate by a single solvolysis process of cellulose. *J. Wood Sci.* **2013**, *59*, 179–182. doi.org/10.1007/s10086-013-1324-8. 765-766
24. Démolis, A.; Eternot, M.; Essayem, N.; Rataboul, F. Influence of butanol isomers on the reactivity of cellulose towards the synthesis of butyl levulinates catalyzed by liquid and solid acid catalysts. *New J. Chem.* **2016**, *40*, 3747–3754. doi.org/10.1039/C5NJ02493E. 767-769
25. Antonetti, C.; Gori, S.; Licursi, D.; Pasini, G.; Frigo, S.; López, M.; Parajó, J.C.; Raspolli Galletti, A.M. One-Pot Alcoholysis of the Lignocellulosic *Eucalyptus nitens* Biomass to *n*-Butyl Levulinate, a Valuable Additive for Diesel Motor Fuel. *Catalysts* **2020**, *10*, 509–530. doi.org/10.3390/catal10050509. 770-772
26. Matrica: green chemicals. Available online: <https://www.matrica.it/Default.asp?ver=en> (accessed on 29 June 2021). 773

27. Mosier, N.; Wyman, C.; Dale, B.; Elander, R.; Lee, Y.Y.; Holtzapple, M.; Ladisch, M. Features of promising technologies for pretreatment of lignocellulosic biomass. *Bioresour. Technol.* **2005**, *96*, 673–686. doi.org/10.1016/j.biortech.2004.06.025. 774–775
28. Cotana, F.; Cavalaglio, G.; Gelosia, M.; Coccia, V.; Petrozzi, A.; Nicolini, A. Effect of Double-Step Steam Explosion Pretreatment in Bioethanol Production from Softwood. *Appl. Biochem. Biotechnol.* **2014**, *174*, 156–167. doi.org/10.1007/s12010-014-1046-4. 776–777
29. (BIT3G) Project – Third generation biorefinery spread on the territory, supported by the Italian Ministry of Education (MIUR) and coordinated by Novamont. 778–779
30. Asghari, F.S.; Yoshida, H. Acid-Catalyzed Production of 5-Hydroxymethyl Furfural from d-Fructose in Subcritical Water. *Ind. Eng. Chem. Res.* **2006**, *45*, 2163–2173. doi.org/10.1021/ie051088y. 780–781
31. Flannelly, T.; Lopes M.; Kupiainen, L.; Dooley, S.; Leahy, J.J. Non-Stoichiometric Formation of Formic and Levulinic Acids from the Hydrolysis of Biomass Derived Hexose Carbohydrates. *RSC Adv.* **2016**, *6*, 5797–5804. doi.org/10.1039/C5RA25172A. 782–783
32. Shi, N.; Liu, Q.; Ju, R.; He, X.; Zhang, Y.; Tang, S.; Ma, L. Condensation of α -carbonyl aldehydes leads to the formation of solid humins during the hydrothermal degradation of carbohydrates. *ACS Omega* **2019**, *4*, 7330–7343. doi: 10.1021/acsomega.9b00508. 784–786
33. Martinez, A.; Rodriguez, M.E.; York, S.W.; Preston, J.F.; Ingram, L.O. Use of UV absorbance to monitor furans in dilute acid hydrolysates of biomass. *Biotechnol. Prog.* **2000**, *16*, 637–641. doi: 10.1021/bp0000508. 787–788
34. Glińska, K.; Lerigoleur, C.; Giralt, J.; Torrens, E.; Bengoa, C. Valorization of cellulose recovered from WWTP sludge to added value levulinic acid with a Brønsted acidic ionic liquid. *Catalysts* **2020**, *10*, 1004–1019. doi:10.3390/catal10091004. 789–790
35. Ibáñez, A.B.; Bauer, S. Analytical method for the determination of organic acids in dilute acid pretreated biomass hydrolysate by liquid chromatography-time-of-flight mass spectrometry. *Biotechnol. Biofuels* **2014**, *7*, 145–153. doi: 10.1186/s13068-014-0145-3. 791–793
36. Iroba, K.L.; Tabil, L.G.; Sokhansanj, S.; Dumonceaux, T. Pretreatment and fractionation of barley straw using steam explosion at low severity factor. *Biomass Bioenergy* **2014**, *66*, 286–300. https://doi.org/10.1016/j.biombioe.2014.02.002. 794–795
37. Schimmelpfennig, S.; Glaser, B. One step forward toward characterization: some important material properties to distinguish biochars. *J. Environ. Qual.* **2012**, *41*, 1001–1013. doi: 10.2134/jeq2011.0146. 796–797
38. Licursi, D.; Antonetti, C.; Bernardini, J.; Cinelli, P.; Coltelli, M.B.; Lazzeri, A.; Martinelli, M.; Raspolli Galletti, A.M. Characterization of the *Arundo Donax* L. solid residue from hydrothermal conversion: comparison with technical lignins and application perspectives. *Ind. Crops Prod.* **2015**, *76*, 1008–1024. https://doi.org/10.1016/j.indcrop.2015.08.007. 798–800
39. Licursi, D.; Antonetti, C.; Fulignati, S.; Vitolo, S.; Puccini, M.; Ribechini, E.; Bernazzani, L.; Raspolli Galletti, A.M. In-depth characterization of valuable char obtained from hydrothermal conversion of hazelnut shells to levulinic acid. *Bioresour. Technol.* **2017**, *244*, 880–888. https://doi.org/10.1016/j.biortech.2017.08.012. 801–803
40. Düdder, H.; Wütscher, A.; Stoll, R.; Muhler, M. Synthesis and characterization of lignite-like fuels obtained by hydrothermal carbonization of cellulose. *Fuel* **2016**, *171*, 54–58. https://doi.org/10.1016/j.fuel.2015.12.031. 804–805
41. Di Fidio, N.; Raspolli Galletti, A.M.; Fulignati, S.; Licursi, D.; Liuzzi, F.; De Bari, I.; Antonetti, C. Multi-Step Exploitation of Raw *Arundo donax* L. for the Selective Synthesis of Second-Generation Sugars by Chemical and Biological Route. *Catalysts* **2020**, *10*, 79–101. doi.org/10.3390/catal10010079. 806–808
42. Fiore, V.; Scalici, T.; Valenza, A. Characterization of a new natural fiber from *Arundo donax* L. as potential reinforcement of polymer composites. *Carbohydr. Polym.* **2014**, *106*, 77–83. https://doi.org/10.1016/j.carbpol.2014.02.016. 809–810
43. Liu, H.M.; Li, H.Y.; Li, M.F. Cornstalk liquefaction in sub- and super-critical ethanol: Characterization of solid residue and the liquefaction mechanism. *J. Energy Inst.* **2017**, *90*, 734–742. https://doi.org/10.1016/j.joei.2016.07.004. 811–812
44. Tsilomelekis, G.; Orella, M.J.; Lin, Z.; Cheng, Z.; Zheng, W.; Nikolakis, V.; Vlachos, D.G. Molecular structure, morphology and growth mechanisms and rates of 5-hydroxymethylfurfural (HMF) derived humins. *Green Chem.* **2016**, *18*, 1983–1993. doi.org/10.1039/C5GC01938A. 813–815
45. Van Zandvoort, I.; Wang, Y.H.; Rasrendra, C.B.; Van Eck, E.R.H.; Bruijninx, P.C.A.; Heeres, H.J.; Weckhuysen, B.M. Formation, molecular structure, and morphology of humins in biomass conversion: influence of feedstock and processing conditions. *ChemSusChem* **2013**, *6*, 1745–1758. doi: 10.1002/cssc.201300332. 816–818
46. Dee, S.J.; Bell, A.T. A study of the acid-catalyzed hydrolysis of cellulose dissolved in ionic liquids and the factors influencing the dehydration of glucose and the formation of humins. *ChemSusChem* **2011**, *4*, 1166–1173. doi.org/10.1002/cssc.201000426. 819–820
47. Antonetti, C.; Raspolli Galletti, A.M.; Fulignati, S.; Licursi, D. Amberlyst A-70: A surprisingly active catalyst for the MW-assisted dehydration of fructose and inulin to HMF in water. *Catal. Commun.* **2017**, *97*, 146–150. doi.org/10.1016/j.catcom.2017.04.032. 821–823
48. Antonetti, C.; Fulignati, S.; Licursi, D.; Raspolli Galletti, A.M. Turning point toward the sustainable production of 5-hydroxymethyl-2-furaldehyde in water: metal salts for its synthesis from fructose and inulin. *ACS Sustain. Chem. Eng.* **2019**, *7*, 6830–6838. doi.org/10.1021/acssuschemeng.8b06162. 824–826
49. Nasir, N.A.; Davies, G.; McGregor, J. Tailoring product characteristics in the carbonisation of brewers' spent grain through-solvent selection. *Food Bioprod. Process.* **2020**, *120*, 41–47. doi: 10.1016/j.fbp.2019.12.010. 827–828
50. Díez, D.; Urueña, A.; Piñero, R.; Barrio, A.; Tamminen, T. Determination of hemicellulose, cellulose, and lignin content in different types of biomasses by thermogravimetric analysis and pseudocomponent kinetic model (TGA-PKM Method). *Processes* **2020**, *8*, 1048–1068. doi: 10.3390/pr8091048. 829–831

-
51. Licursi, D.; Antonetti, C.; Mattonai, M.; Pérez-Armada S. Rivas, L.; Ribechini, E.; Raspolli Galletti, A.M. Multi-valorisation of giant reed (*Arundo Donax* L.) to give levulinic acid and valuable phenolic antioxidants. *Ind. Crop. Prod.* **2018**, *112*, 6-17. doi: 10.1016/j.indcrop.2017.11.007. 832
833
52. Yu, L.; Falco, C.; Weber, J.; White, R.J.; Howe, J.Y.; Titirici, M.M. Carbohydrate-derived hydrothermal carbons: A thorough characterization study. *Langmuir* **2012**, *28*, 12373-12383. doi: 10.1021/la3024277. 834
835
836
53. Rasrendra, C.B.; Windt, M.; Wang, Y.; Adisasmito, S.; Makertihartha, I.G.B.N.; Van Eck, E.R.H.; Meier, D.; Heeres, H.J. Experimental studies on the pyrolysis of humins from the acid-catalysed dehydration of C6-sugars. *J. Anal. Appl. Pyrolysis* **2013**, *104*, 299-307. doi: 10.1016/j.jaap.2013.07.003. 837
838
839
54. Antonetti, C.; Licursi, D.; Raspolli Galletti, A.M. New intensification strategies for the direct conversion of real biomass into platform and fine chemicals: What are the main improvable key aspects? *Catalysts* **2020**, *10*, 961-974. doi: 10.3390/catal10090961. 840
841
55. Jindo, K.; Sánchez-Monedero, M.A.; Mastrolonardo, G.; Audette, Y.; Higashikawa, F.S.; Silva, C.A.; Akashi, K.; Mondini, C. Role of biochar in promoting circular economy in the agriculture sector. Part 2: A review of the biochar roles in growing media, composting and as soil amendment. *Chem. Biol. Technol. Agric.* **2020**, *7*, 16-25. doi: 10.1186/s40538-020-00179-3. 842
843
844
56. Liu, W.J.; Jiang, H.; Yu, H.Q. Development of biochar-based functional materials: Toward a sustainable platform carbon material. *Chem. Rev.* **2015**, *115*, 12251-12285. doi: 10.1021/acs.chemrev.5b00195. 845
846
57. a) Sluiter, A.; Hames, B.; Ruiz, R.; Scarlata, C.; Sluiter, J.; Templeton, D.; Crocker, D. Determination of Structural Carbohydrates and Lignin in Biomass. Laboratory Analytical Procedure (LAP), NREL/TP-510-42618, 2008; b) Sluiter, A.; Ruiz, R.; Scarlata, C.; Sluiter, J.; Templeton, D. Determination of Extractives in Biomass. Laboratory Analytical Procedure (LAP), NREL/TP-510-42619, 2008; c) Sluiter, A.; Hames, B.; Ruiz, R.; Scarlata, C.; Sluiter, J.; Templeton, D. Determination of Ash in Biomass. Laboratory Analytical Procedure (LAP), NREL/TP-510-42622, 2008. 847
848
849
850
851
58. Sluiter, A.; Hames, B.; Hyman, D.; Payne, C.; Ruiz, R.; Scarlata, C.; Sluiter, J.; Templeton, D.; Wolfe, J. Determination of Total Solids in Biomass and Total Dissolved Solids in Liquid Process Samples. Laboratory Analytical Procedure (LAP), NREL/TP-510-42621, 2008. 852
853
854
59. Channiwala, S.A.; Parikh, P.P. A unified correlation for estimating HHV of solid, liquid and gaseous fuels. *Fuel* **2002**, *81*, 1051-1063. doi: 10.1016/S0016-2361(01)00131-4. 855
856